

Magnetic properties of NiCu thin films obtained by electrodeposition

D. BAZAVAN, R. BAZAVAN, I. ENCULESCU^a, E. MATEI^a, C. NECULA, L. ION, S. ANTOHE^{b*}

Faculty of Physics, University of Bucharest, 405 Atomistilor, P.O. Box MG-11, 077125, Magurele-Ilfov, Romania

^a*National Institute for Materials Physics, 105b Atomistilor, P.O. Box MG-7, 077125, Magurele-Ilfov, Romania*

^b*Horia Hulubei Foundation, 407 Atomistilor, P.O.Box MG-11, 077125, Romania*

Using an electrochemical method have been produced NiCu thin films for magnetic applications. The recent development of first-order reversal curve (FORC) diagrams has allowed the detailed investigation of coercivity spectra, interaction and domain states of magnetic thin films. Their magnetic properties have been investigated by Micro MagTM 3900 Vibrating Sample Magnetometer (VSM) and are discussed.

(Received April 03, 2009; accepted after revision May 25, 2009)

Keywords: NiCu, FORC, Magnetic properties

1. Introduction

In many different fields of science and engineering the hysteresis curves are used for characterizing the magnetic properties of natural and synthetic materials. A typical hysteresis curve may consist of several hundred data points. This data provide information about the magnetic properties of the material, but recently the researchers have developed a technique that allows them to determine the distribution of magnetic properties within material [1, 2]. This technique uses partial hysteresis curves to produce a First-Order Reversal Curve (or FORC) diagram. On a FORC diagram, each magnetic system exhibits a “signature” which contains detailed information about that system’s magnetic properties [3-8]. More information, such as details about the composition and size distribution of the magnetic particles and their interactions can be obtained by using a FORC than a single hysteresis curve.

In this paper we report on the results of an investigation on magnetic properties of NiCu thin films obtained by electrodeposition, using the FORC diagram analysis. Such a study is justified by the potential applications of NiCu thin films for magnetic field sensors [9], giant magnetoresistance systems, in magnetic recording as MRAM, HDD etc.

2. FORC diagram

The measurement of a FORC begins with the saturation of the sample in a positive applied field, H_+ (figure 1). This field is decreased to a reversal field H_a . The FORC consist in measurement of magnetization as the field is then increased from H_a back up to saturation. On the FORC with reversal point H_a the magnetization at applied field H_b is denoted by $M(H_a, H_b)$, where $H_b \geq H_a$.

The FORC distribution is determined by using data from consecutive measurement points on consecutive reversal curve, which is defined as the mixed second derivative:

$$\rho(H_a, H_b) = -\frac{1}{2} \frac{\partial^2 M(H_a, H_b)}{\partial H_a \partial H_b} \quad (1)$$

where $\rho(H_a, H_b)$ is well defined for $H_b > H_a$.

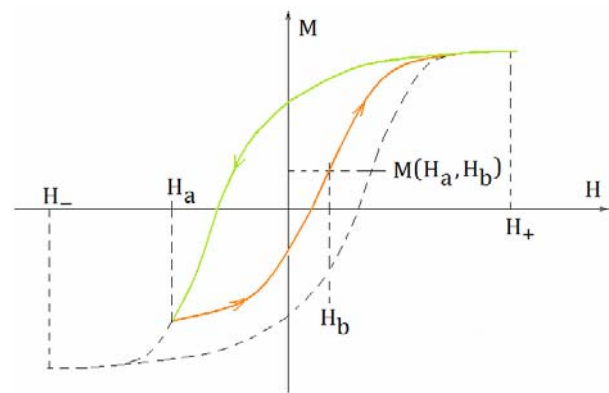


Fig. 1. Definition of a first-order reversal curve (FORC): green line is the descending magnetization curve taken from a positive saturating field H_+ to some field H_a ; red line is the first order reversal curve (FORC) from H_a returning to saturation [2].

When is plotted the FORC distribution, it is convenient to rotate axes by changing the FORC distribution coordinates from $\{H_a, H_b\}$ to $\{H_u = (H_a + H_b)/2, H_c = (H_b - H_a)/2\}$.

A FORC diagram is a contour plot of a FORC distribution with H_c and H_u on the horizontal and vertical axes, respectively [10].

3. Experimental results and discussion

NiCu magnetic thin films were obtained by using an electrodeposition method. The films were electrodeposited in a Watts bath. The composition of the basic plating solution was: nickel sulphate hexahydrate (225 g/l), nickel chloride hexahydrate (30 g/l), boric acid (22,5 g/l) and copper sulphate pentahydrate (4 g/l). An organic additive (PVP – polyvinyl pyrrolidone, 5 g/l) was used as wetting agent.

As a first step of the deposition procedure, a gold thin film, 50 nm thick, was sputtered on the surface of the glass substrate. The gold film was subsequently used as working electrode during the deposition of the magnetic alloy. The electrochemical deposition was performed by using a VoltaLab potentiostat controlled by a computer. The temperature was kept constant, at 65° C. A three electrode configuration was used, with a platinum counterelectrode and a commercial saturated calomel electrode (SCE) as reference. During the deposition, the electrolytic bath was mechanical stirred for homogenization.

Three successive polarization curves, recorded during deposition, are shown in Fig. 2.

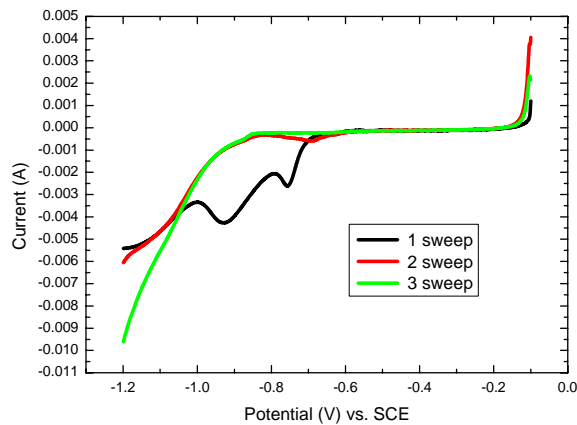
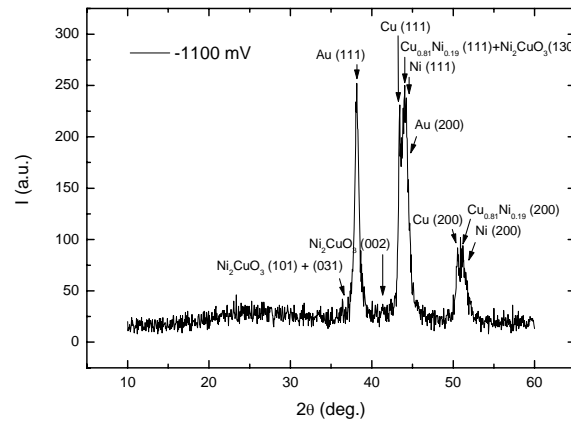
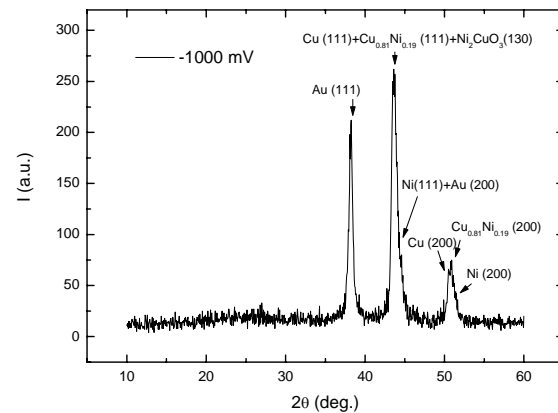


Fig. 2. Voltammetric curves recorded during the deposition of NiCu thin films, in the conditions specified in text.

The flat region extending from -200 mV to -850 mV is associated with a stoichiometric compound deposition, while the region from -850 mV to -1200 mV is associated with the prevalent deposition of the element which has a higher concentration in the bath (Ni + NiCu). There are not significant differences between the second and the third runs, hence the deposition process does not depend essentially on the substrate material.



(a)



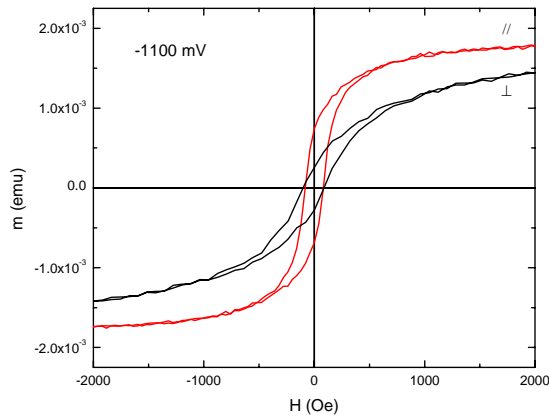
(b)

Fig. 3. Experimental X-ray diffraction patterns of the NiCu analyzed samples.

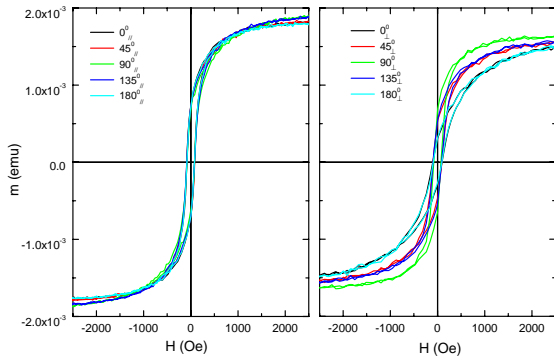
The crystallinity of the films was characterized by X-ray diffraction (XRD), using a high resolution X-ray diffractometer (D8 Discover – Bruker).

XRD spectra were recorded by using Cu- $K_{\alpha 1}$ line, $\lambda = 1.5406 \text{ \AA}$, in a grazing incidence geometry for increasing the path length of the X-ray beam through the film. XRD patterns are shown in figure 3. A richer structure of the diffraction peaks can be seen in the case of the sample electrodeposited at -1100 mV vs. SCE (see Fig. 3(a)). There is evidence for the presence of a $\text{Cu}_{0.81}\text{Ni}_{0.19}$ phase in the analyzed film. Also the peaks due to reflections on (111) planes of Au, Cu and Ni separate phases can be clearly seen. In the case of the sample deposited at -1000 mV vs. SCE (shown in Fig. 3(b)), the diffraction peaks are featureless, although suggesting the presence of the same crystalline phases, with an increased content of Cu, as a separate phase.

The hysteresis curves and the FORC distributions were recorded by using Micro Mag™ 3900 Vibrating Sample Magnetometer (VSM) from Princeton Measurements Corporation. The hysteresis curves for NiCu samples are shown in Figs. 4 and 5, and the FORC distribution in Figs. 7 and 9, respectively.



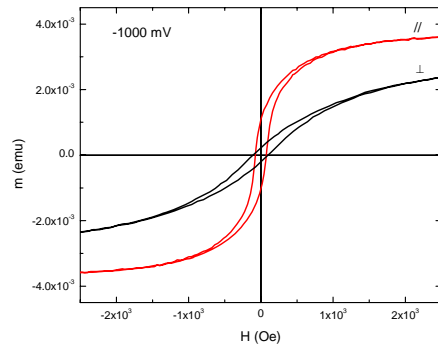
(a)



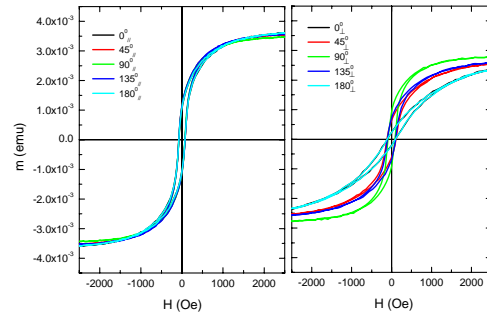
(b)

Fig. 4. (a) VSM magnetization loops of NiCu sample obtained at -1100 mV and (b) VSM magnetization loops obtained at different orientation of magnetic field.

The standard hysteresis properties are M_r – the remanence magnetization, M_s – the saturation magnetization, H_c – the coercivity or switching field and H_{cr} – the coercivity of remanence (a field that reduce the remanence magnetization to zero after it is applied and removed).



(a)



(b)

Fig. 5. (a) VSM magnetization loops of NiCu sample obtained at -1000 mV and (b) VSM magnetization loops obtained at different orientation of magnetic field.

For hysteresis loops are evidenced two type of shapes. First type belonging to parallel applied field is „wasp-waisted”, indicating SD-MD mixture. Second type belonging to perpendicular applied field is larger, having more pronounced S shape.

The hysteresis curves revealed that the samples shows anisotropy and the shapes of hysteresis loops indicating PSD populations.

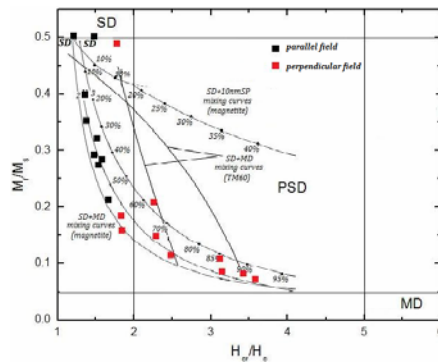


Fig. 6. Hysteresis data of the NiCu samples compared with theoretical mixing curves developed by [12]. SD – single domain, PSD – pseudo-single domain and MD – multidomain.

The ratio of M_r/M_s and H_{cr}/H_c yield information of magnetic domain [11]. To estimate domain state we use Day plot (M_r/M_s versus H_{cr}/H_c , [11]). For parallel applied field M_r/M_s ranges from 0.2798 to 0.4993 and H_{cr}/H_c varies between 1.2159 to 1.662. For perpendicular applied field M_r/M_s ranges from 0.085 to 0.4889 and H_{cr}/H_c varies between 1.7754 to 3.5797. Judging from these values, it seems that almost all the samples fall in pseudo-single domain (PSD) grain size region, probably indicating a mixture of multidomain (MD) and a significant amount of single domain (SD) grains [11] (Fig. 6).

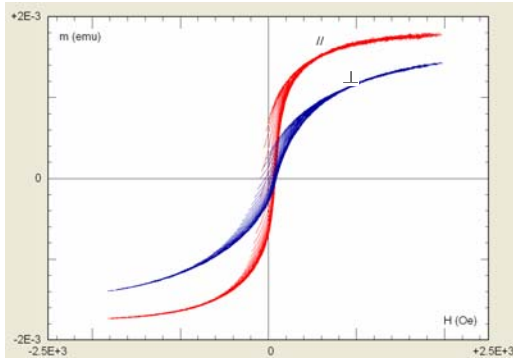


Fig. 7. FORCs distribution for NiCu sample obtained at -1100 mV.

The FORCs (Fig. 7) can be transformed into the contour plot (figure 8), which we will refer to as a FORC diagram.

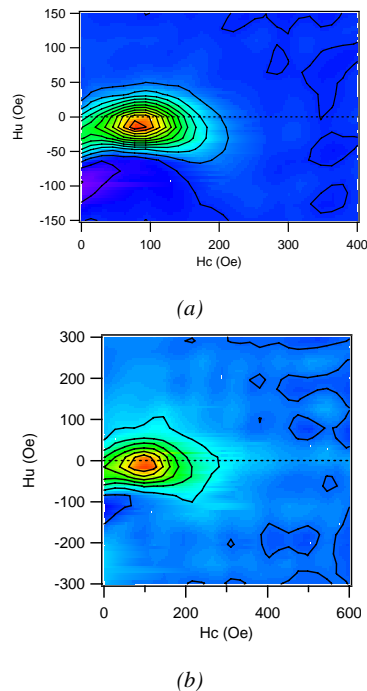


Fig. 8. FORC diagrams for NiCu sample obtained at -1100 mV: (a) parallel to magnetic field and (b) perpendicular to magnetic field.

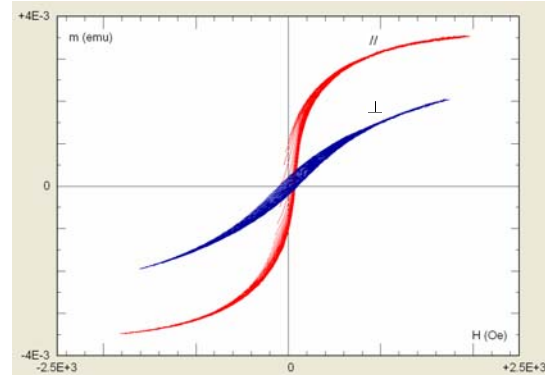


Fig. 9. FORCs distribution for NiCu sample obtained at -1000 mV.

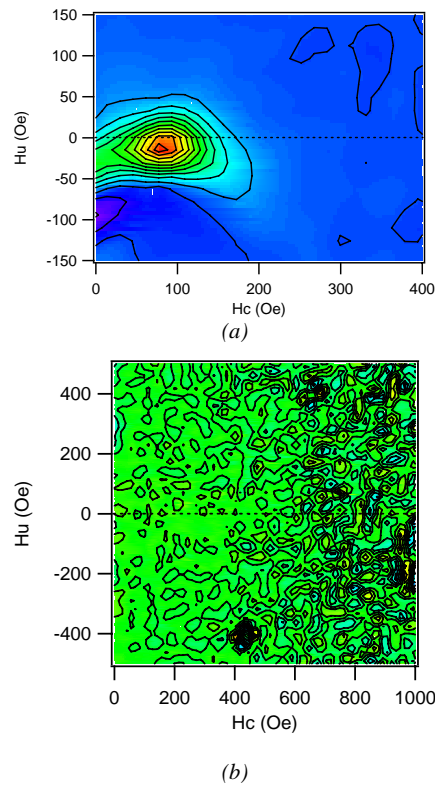


Fig. 10. FORC diagrams for NiCu sample obtained at -1000 mV: (a) parallel to magnetic field and (b) perpendicular to magnetic field.

To construct a FORC diagram, 111 first-order reversal curves were measured. The FORC data processing was performed using FORCinel software developed by [13]. This FORC diagrams confirm that almost all the samples fall in pseudo-single domain (PSD) grain size region.

4. Conclusions

Using an electrodeposition method, NiCu magnetic thin films were prepared. An investigation on the magnetic properties of the layers was performed. XRD was used to

investigate the crystallinity of obtained structures. The XRD analysis revealed that all NiCu thin films were polycrystalline. Electrodeposition at more negative potentials results in films richer in Ni, present either in a $\text{Cu}_{0.81}\text{Ni}_{0.19}$ crystalline phase or as a separate elemental phase. Hysteresis curves and FORC diagrams have shown that the magnetic domain state is compatible with SD-MD mixture. It seems that almost all the samples fall in pseudo-single domain (PSD) grain size region, probably indicating a mixture of multidomain (MD) and a significant amount of single domain (SD) grains [11].

References

- [1] C. R. Pike, A. P. Roberts, K. L. Verosub, *J. Appl. Phys.* **85**, 6660 (1999).
- [2] A. P. Roberts, C. R. Pike, K. L. Verosub, *J. Geophys. Res.* **105**, 28461 (2000).
- [3] C. R. Pike, C. A. Ross, R. T. Scalettar, G. Zimanyi, *Phys. Rev. B* **71**, 134407 (2005).
- [4] C. R. Pike, A. P. Roberts, K. L. Verosub, *Geophys. J. Int.* **145**, 721, 2001.
- [5] C. R. Pike, A. P. Roberts, M. J. Dekkers, K. L. Verosub, *Phys. Earth Planet. Inter.* **126**, 11 (2001).
- [6] H. G. Katzgraber, F. Pazmandi, C. R. Pike, K. Liu, R. T. Scalettar, K. L. Verosub, G. T. Zimanyi, *Phys. Rev. Lett.* **89**, 257202 (2002).
- [7] A. R. Muxworthy, D. J. Dunlop, *Earth Planet. Sci. Lett.* **203**, 369 (2002).
- [8] A. Stancu, C. R. Pike, L. Stoleriu, P. Postolache, D. Cimpoesu, *J. Appl. Phys.* **93**, 6620 (2003).
- [9] I. Giouroudi, C. Orfanidou, E. Hristoforu, *Sensors and Actuators A: Physical* **106**(1), 2003.
- [10] I. D. Mayergoyz, *IEEE Trans. Magn.* **MAG-22**, 603 (1986).
- [11] R. Day, M. Fuller, V.A. Schmidt, *Phys. Earth Planet. Int.* **13**, 260 (1977).
- [12] D. J. Dunlop, *J. Geophys. Res.* **107**(B3), 2056 (2002).
- [13] R. J. Harrison, J. M. Feinberg, *Geochemistry, Geophysics, Geosystems* **9**, Q05016 (2008), doi:10.1029/2008GC001987.

*Corresponding author: santohe@solid-fizica.unibuc.ro